Production cross-section of ^{53}Mn via different reaction channels**

Navita Kanyal,[1,*] Bhawna Pandey,[1] Jyoti Pandey,[1] P.V. Subhash,[2] S. Vala,[3] Rajnikant Makwana,[4] S.V. Suryanarayana[5] and G.C. Joshi[6]

[1] *Department of Physics, G.B. Pant University of Agriculture and Technology, Pantnagar, Uttarakhand (U.K.) 263145, India*

[2] *Institute for Plasma Research, HBNI, ITER-India, Gandhinagar, Gujarat 382428, India*

[3] *Institute for Plasma Research, Fusion Neutronics Laboratory, Gandhinagar, Gujarat 382428, India*

[4] *Physics Department, Faculty of Science, M.S. University of Baroda, Vadodara, Gujarat 390002, India*

[5] *Nuclear Physics Division, Bhabha Atomic Research Centre, Mumbai, Maharashtra 400085, India*

[6] *Radiations and Isotopic Tracers Laboratory, Department of Physics, G.B.Pant University of Agriculture and Technology, Pantnagar, Uttarakhand 263145, India*

Long-lived activation products produced during the operation of fusion reactors may engender long-term waste disposal problems along with radiation damage. ^{53}Mn ($t_{1/2}$ = 3.7 Myear) is a long-lived radionuclide produced inside a fusion reactor via different pathways. Production cross-sections of ^{53}Mn through neutron-induced reaction on stable nuclides via ^{54}Fe(n,np)^{53}Mn, ^{54}Fe(n,2n)^{53}Fe(β^+)^{53}Mn, ^{54}Fe(n,d)^{53}Mn reactions, on unstable nuclei via ^{54}Mn(n,2n)^{53}Mn, ^{55}Fe(n,t)^{53}Mn and ^{57}Co(n,nα)^{53}Mn reactions, and by sequential charged particle-induced reactions ^{50}V(α,n)^{53}Mn, ^{53}Cr(p,n)^{53}Mn, ^{52}Cr(d,n)^{53}Mn have been calculated in an energy range from threshold to 20 MeV using TALYS-1.9. Sequential charged particle-induced reactions make a significant contribution to the production of ^{53}Mn inside a fusion reactor. Outgoing particle (ejectile) energy spectra show the presence of a high energy tail due to a pre-equilibrium contribution to charged particle reactions. Existing experimental data for the reactions cosidered are scarce and contradictory in the EXFOR data library, which is why these reactions are studied in the present work. Nuclear data related to the production of ^{53}Mn via different reactions are briefly discussed.

* Corresponding author. E-mail: navitakanyal@gmail.com

** This paper was first presented at the International Conference on Advanced Materials, Energy & Environmental Sustainability (ICAMEES-2018), 14–15 December 2018 in Dehradun, India.

Nanotechnology Perceptions **15** (2019) 150–161
Received 27 January 2019; *accepted* 31 July 2019

doi: 10.4024/N09KA19A.ntp.15.02

1. Introduction

Production cross-sections for long-lived target and residual nuclei are of great importance for the development of low-activation materials in a fusion reactor. Cr, Fe, Ni and V are the main elements suitable for structural and blanket components in the reactor. One aim of fusion energy research is to cut down the radiological risk. Radioactive products are not produced directly from fusion fuel cycles, but the neutron and charged particles like the proton, deuteron and triton produced in fusion reactions do engender radioactivity in the surrounding reactor structural material [1–3]. In the build-up of radioactivity, nuclides with relatively long half-lives are the main hazards. With time, their activity becomes dominant. Radioactive wastes from nuclear reactor operation can contain long-lived radionuclides [4]. Prediction of the radioactive decay characteristics of reactor components is very important for the safety of operators, for planning maintenance schedules and routes, and for knowing the amount and type of waste for disposal [5]. Many long-lived activation products produced during the service of a fusion reactor may cause long-term waste disposal problems along with radiation damage.

The radionuclide ^{53}Mn ($t_{1/2}$ = 3.7 Myear) is produced inside a nuclear reactor via different channels; it decays into ^{53}Cr via electron capture. The production of this long-lived radionuclide is of considerable import for fusion technology because radionuclides with half-lives of less than 10^9 years are potential waste disposal hazards [1]. The activity of ^{53}Mn will increase steadily during the lifetime of an operating reactor and may complicate the ultimate disposal of manganese.

Existing experimental cross-section data for the production of ^{53}Mn via neutron- as well as sequential charged particle-induced reaction are scarce and discordant [6]. Experimental determination of cross-sections for unstable (with a very short half-life) and long-lived radionuclides involves great difficulty. In a typical fusion reactor deuterium (D) and tritium (T) fuse together and produce high-energy neutrons (~14.6 MeV). In order to estimate the production of ^{53}Mn in the D–T fusion environment, an accurate excitation function for $^{54}Fe(n,np)^{53}Mn$, $^{54}Fe(n,2n)^{53}Fe(\beta^+)^{53}Mn$, $^{54}Fe(n,d)^{53}Mn$, $^{54}Mn(n,2n)^{53}Mn$, $^{55}Fe(n,t)^{53}Mn$ and $^{57}Co(n,n\alpha)^{53}Mn$, $^{50}V(\alpha,n)^{53}Mn$, $^{53}Cr(p,n)^{53}Mn$, $^{52}Cr(d,n)^{53}Mn$ is necessary. This then allows one to make accurate predictions of the build-up of ^{53}Mn and its significance for long-term waste disposal.

In the present investigation, all possible reaction channels by which ^{53}Mn can be generated inside a fusion reactor have been studied. There is a need to study the production cross-section of ^{53}Mn via the nuclear reaction $^{54}Mn(n,2n)^{53}Mn$ [7], where there exist many pathways through which ^{53}Mn may be produced. Broadly, the pathways of production of ^{53}Mn can be ordered into three categories: (a) neutron-induced reactions of stable nuclei (^{54}Fe); (b) neutron-induced reactions on unstable nuclei [^{54}Mn ($t_{1/2}$=312.03 days), ^{55}Fe ($t_{1/2}$= 2.73 yr), ^{57}Co ($t_{1/2}$=271.79 days)]; and (c) sequential charged particle-induced (x,n) reaction. The various neutron-induced pathways for the production of ^{53}Mn are shown in Fig. 1. Neutrons inside the nuclear reactor have an energy of about 14.6 MeV but interact with other reactor materials whereupon their energy degrades and hence the neutron spectrum is found in an energy range from 1 MeV to 14 MeV [2]. Therefore, it is important to study neutron-induced reactions like (n,p), (n,2n), (n,np), (n,nd), (n,t), (n,α) etc. in this energy range, where n, p, d, t and α represent neutron, proton, deuteron, triton and alpha particle, respectively.

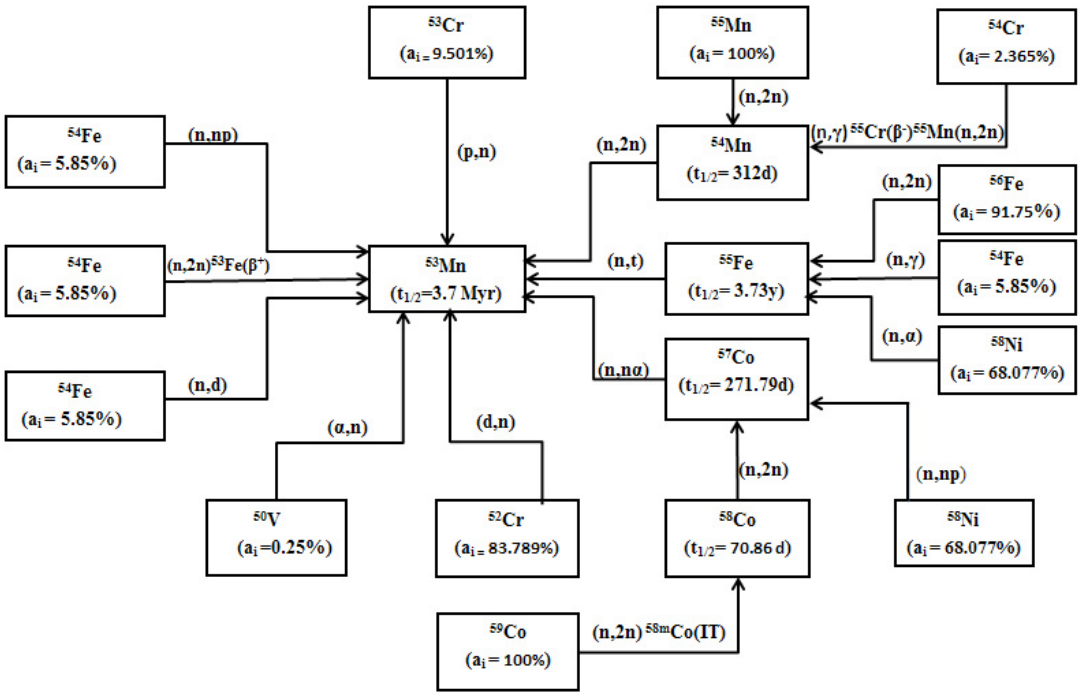

Figure 1. Schematic of ^{53}Mn formation pathways in a typical fusion reactor.

In sequential reactions, charged particles are produced in the first step due to neutron-induced reaction A(n,x)B, where x represents a neutron or a charged particle (p, d, t, α), and subsequently the emitted charged particles react with target material as well as other materials via A(x,n)C or D(x,n)E, producing residual nuclei C or E. Primary neutron interaction with reactor materials leads to the interaction of their product particles with various reactor materials, which is followed by the production of large amounts of residual unstable nuclei, which decay by emission of α, β, γ and X-rays [8]. The production of radioactivity via sequential reaction severely influences total induced activity in the following two cases: (1) sequential reactions produce undesirable long-lived radioactive nuclei in low-activation materials; and (2) charged particles emitted from another material nearby promote sequential reactions in a local boundary region [9].

The main aim of this work is to check the predictive power of TALYS-1.9 to calculate the unknown cross-sections for some important reactions producing ^{53}Mn. This aim was achieved by evaluating the consistency of the calculation method, and cross-checking the parameters used with available experimental data and the trend of the calculated results across the range of incident energies.

2. Nuclear model calculation

The model calculations for $^{54}Fe(n,np)^{53}Mn$, $^{54}Fe(n,2n)^{53}Fe(\beta^+)^{53}Mn$, $^{54}Fe(n,d)^{53}Mn$, $^{54}Mn(n,2n)^{53}Mn$, $^{55}Fe(n,t)^{53}Mn$, $^{57}Co(n,n\alpha)^{53}Mn$, $^{50}V(\alpha,n)^{53}Mn$, $^{52}Cr(d,n)^{53}Mn$ and $^{53}Cr(p,n)^{53}Mn$

were carried out using TALYS-1.9 [10], a program for simulating nuclear reactions in the incident energy range from 1 keV to 200 MeV. It is based on a collection of nuclear models, put into a single code system, and typically in a few seconds it can generate nuclear data for all open reaction channels, according to a user-defined energy and angle grid. The main uses of this model are: as a nuclear physics tool; for comparing nuclear models with experimental data; and for obtaining nuclear data where no experimental data exist. We used it in the neutron energy range from threshold (E_{th}) to 20 MeV. The incident particles were gamma rays, neutrons, protons, deuterons, triton, ^{3}He and alpha particles for target nuclei of mass 12 and heavier. The cross-section of the compound nuclear reactions are calculated using the Hauser–Feshbach statistical model with pre-equilibrium [11]. All required inputs were taken from the Reference Input Parameter Library (RIPL) [12].

3. Results and discussion

The calculated cross-section data for all reactions considered together with experimental values taken from the EXFOR data library, and the data from the ENDF/B-VII.1, TENDL-2017 and FENDL-3.1c libraries, are shown in Figs 2–16.

There are very few experimental measurements for the production of ^{53}Mn. The main problem for the measurement of such a type of reaction cross-section is the very long half-life ($\tau_{1/2}$) of the daughter nuclei, hence the activation technique cannot be used. Furthermore, in some cases the target itself is not stable because direct experimental measurement is not possible in the laboratory. To understand the production of ^{53}Mn via different pathways the present results are categorized into three sub-sections.

(a) Production of ^{53}Mn via neutron-induced reaction of the stable nucleus ^{54}Fe

There are three pathways, viz. ^{54}Fe(n,np) (E_{th}= 9.018 MeV), ^{54}Fe(n,d) (E_{th}= 6.752 MeV) and by a β^{+} decay of ^{53}Fe ($\tau_{1/2}$= 8.51 min) produced via the ^{54}Fe(n,2n) (E_{th}= 13.628 MeV) reaction. All three reactions take place around 10 MeV. Calculated reaction cross-sections are shown in Figs 2–6 together with experimental data from EXFOR and data available in TENDL-2017, ENDF/B-VII.1, FENDL-3.1c and EAF-2010. In all three reactions, ^{54}Fe(n,np) is the major reaction channel by which ^{53}Mn can be produced inside the reactor, while the reactions of ^{54}Fe(n,d) and ^{54}Fe(n,2n) contribute less compared to the ^{54}Fe(n,np) reaction. To check the reaction mechanism, the outgoing energy spectrum of neutrons and protons ejected during the ^{54}Fe(n,np) reaction has also been studied. ^{54}Fe(n,np)^{53}Mn reactions proceed predominantly via compound nucleus decay. Wallner et al. (2011) measured the production cross-section of ^{53}Mn via the combined reactions, viz. ^{54}Fe(n,np+d)^{53}Mn+^{54}Fe(n,2n)^{53}Fe. Fig. 6. shows a comparison of the TALYS-1.9 calculation with the combined production cross-section of ^{53}Mn given by Wallner et al.

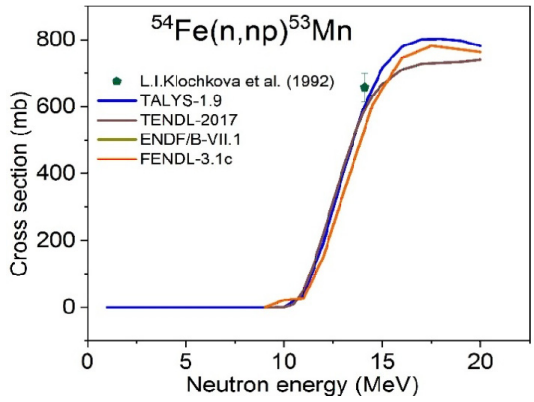

Figure 2. Calculated excitation function of $^{54}Fe(n,np)^{53}Mn$ along with data from various libraries.

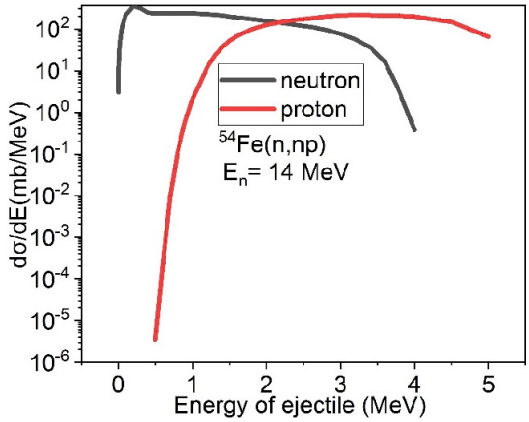

Figure 3. Calculated outgoing particle energy spectra for $^{54}Fe(n,np)^{53}Mn$.

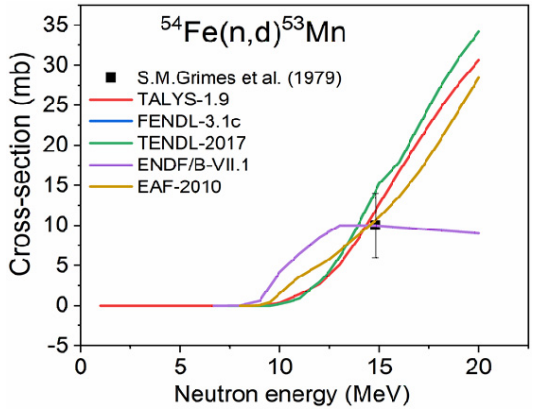

Figure 4. Calculated excitation function of $^{54}Fe(n,d)^{53}Mn$ along with data from various libraries.

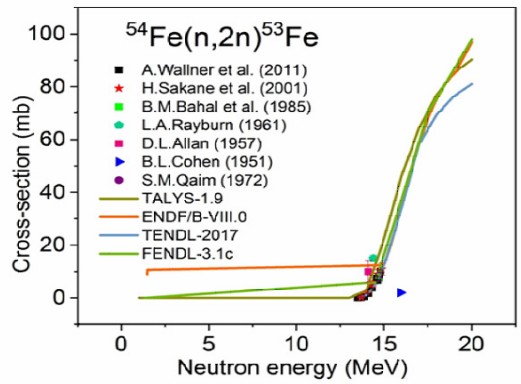

Figure 5. Calculated excitation function of $^{54}Fe(n,2n)^{54}Fe$ along with data from various libraries.

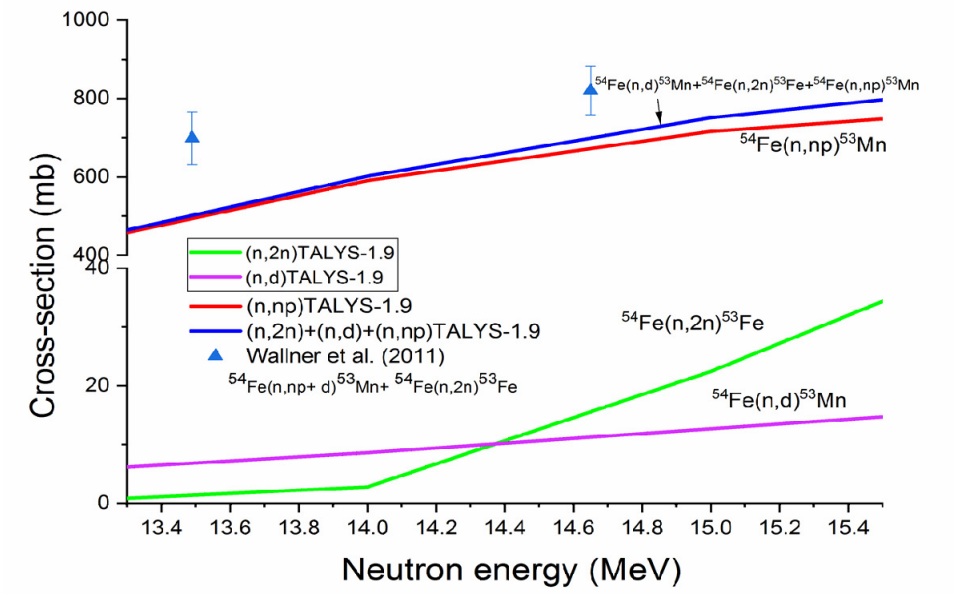

Figure 6. Total production cross-section of ^{53}Mn via $^{54}Fe(n,d)$, $^{54}Fe(n,2n)$, $^{54}Fe(n,np)$ with nuclear model calculation and comparison with Wallner et al.'s (2011) experimental data [6].

(b) Production of ^{53}Mn via neutron -induced reaction of unstable nuclei ^{54}Mn ($t_{1/2}$=312.3 days), ^{55}Fe ($t_{1/2}$=2.73 y), ^{57}Co ($t_{1/2}$=271.79 days)

Production cross-sections of the ^{53}Mn via $^{54}Mn(n,2n)$ (E_{th}= 9.106 MeV), $^{55}Fe(n,t)$ (E_{th}= 9.847 MeV) and $^{57}Co(n,n\alpha)$ (E_{th}= 7.205 MeV) reactions are plotted in Figs 7–10 along with the evaluated data available in the TENDL-2017,ENDF/B-VII.1 and EAF-2010 libraries. Since the unstable nuclei ^{54}Mn ($\tau_{1/2}$ = 312 days), ^{55}Fe ($\tau_{1/2}$ = 3.73 years) and ^{57}Co ($\tau_{1/2}$ = 271.79 days) are not available in nature, there is no experimental measurement for the $^{54}Mn(n,2n)^{53}Mn$,$^{55}Fe(n,t)^{53}Mn$ and $^{57}Co(n,\alpha)^{53}Mn$ reactions. Experimental measurement of such types of reaction can be performed by a surrogate method [2], whereby unstable

radioactive nuclei are produced inside the reactor after transmutation through neutron-induced reactions of stable nuclei such as iron, nickel, chromium or cobalt, which are already present in a fusion reactor material. As shown in Fig. 1, the main reactions for the production of ^{54}Mn inside nuclear reactors are $^{54}Cr(n,\gamma)^{55}Cr(\beta^-)^{55}Mn(n,2n)^{54}Mn$ and $^{55}Mn(n,2n)^{54}Mn$. ^{55}Fe is produced via the $^{56}Fe(n,2n)^{55}Fe$, $^{54}Fe(n,\gamma)^{55}Fe$ and $^{58}Ni(n,\alpha)^{55}Fe$ reactions while ^{57}Co is produced via the $^{59}Co(n,2n)^{58m}Co(IT)^{58}Co(n,2n)^{57}Co$ and $^{58}Ni(n,np)^{57}Co$ reactions.

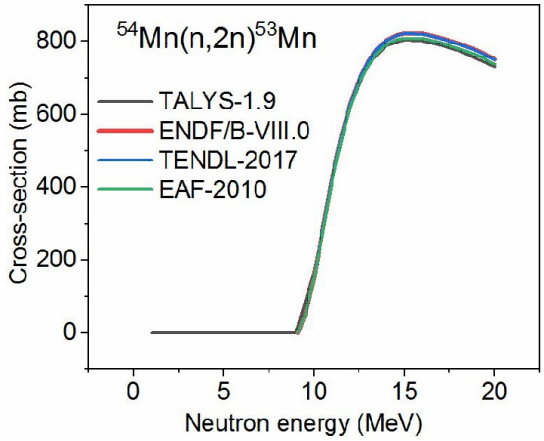

Figure 7. Calculated excitation function of $^{54}Mn(n,2n)^{54}Mn$ along with data from various libraries.

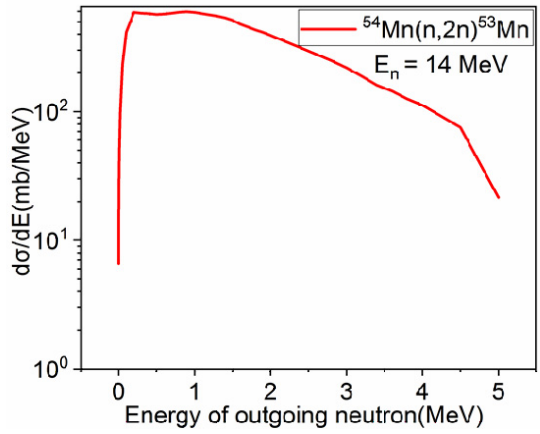

Figure 8. Calculated outgoing particle energy spectra for $^{54}Mn(n,2n)^{53}Mn$.

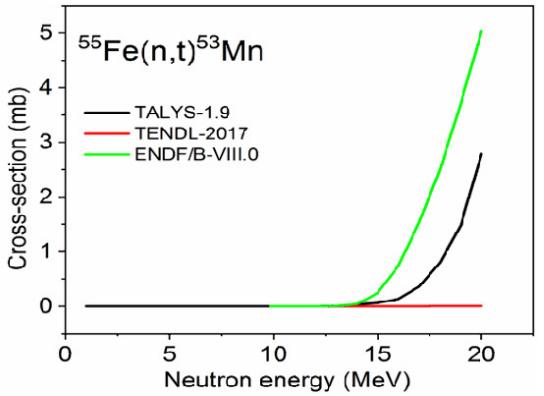

Figure 9. Calculated excitation function of $^{55}Fe(n,t)^{53}Mn$ along with data from various libraries.

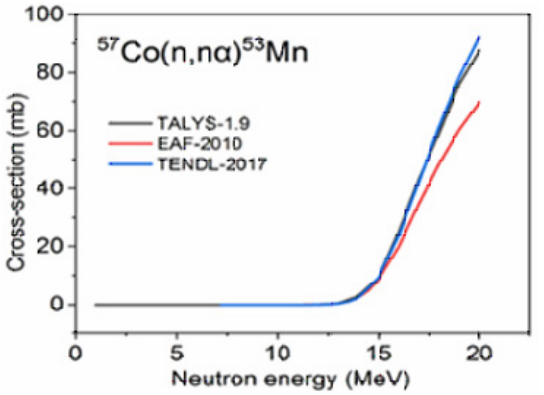

Figure 10. Calculated excitation function of $^{57}Co(n,n\alpha)^{53}Mn$ along with data from various libraries.

(c) Production of ^{53}Mn via sequential charged-particle reactions of ^{50}V, ^{52}Cr, ^{53}Cr

The production cross-sections of ^{53}Mn via $^{50}V(\alpha,n)$ (E_{th}= 0.194 MeV), $^{52}Cr(d,n)$ (E_{th}= 0 MeV) and $^{53}Cr(p,n)$ (E_{th}= 1.405MeV) are shown in Figs 11–16. There is no data available for the $^{50}V(\alpha,n)^{53}Mn$ and $^{52}Cr(d,n)^{53}Mn$ reactions in EXFOR nor in the evaluated data libraries. In the case of the $^{53}Cr(p,n)^{53}Mn$ reaction, very little experimental data is available, and only at low energies from 1.4 to 5.88 MeV. In Figs 11, 13 and 15 the bell-like shape of the excitation curve, which is characteristic of compound nucleus formation, rises abruptly above the reaction threshold and descends due to other competing channels. The pre-equilibrium contribution increases with increasing energy of the projectile. In Figs 12, 14 and 16 the outgoing particle energy spectra ($d\sigma/dE$) are plotted to see the reaction mechanism. The low-energy part shows Maxwellian behaviour (compound nuclear reaction mechanism), and the high-energy tail shows the contribution from the pre-equilibrium reaction mechanism.

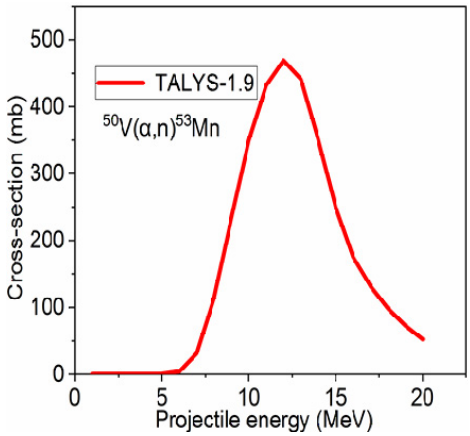

Figure 11. Calculated excitation function of $^{50}V(\alpha,n)^{53}Mn$.

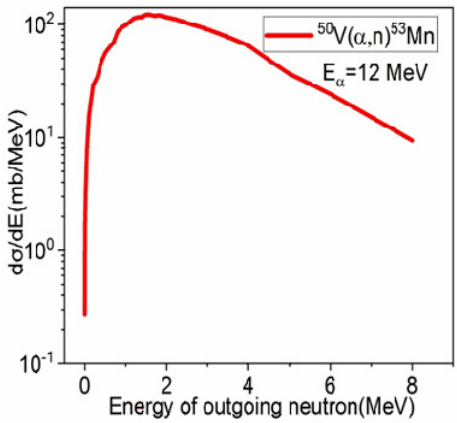

Figure 12. Calculated outgoing particle energy spectrum for $^{50}V(\alpha,n)^{53}Mn$

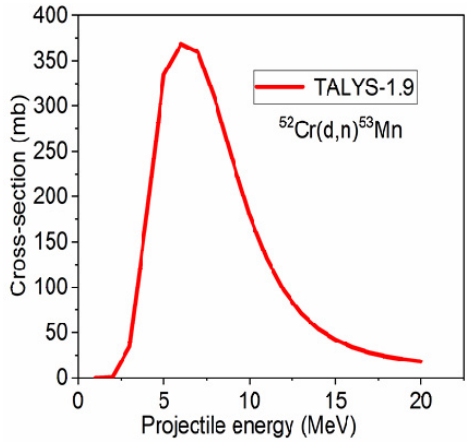

Figure 13. Calculated excitation function of $^{52}Cr(d,n)^{53}Mn$.

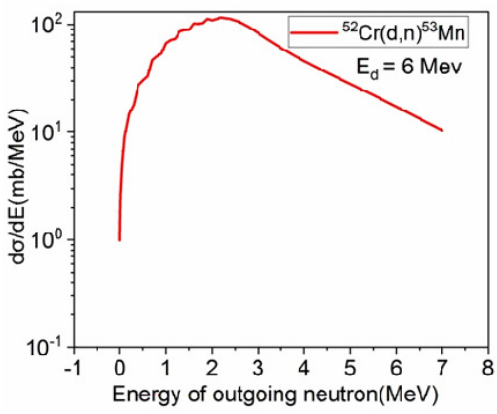

Figure 14. Calculated excitation function of $^{52}Cr(d,n)^{53}Mn$.

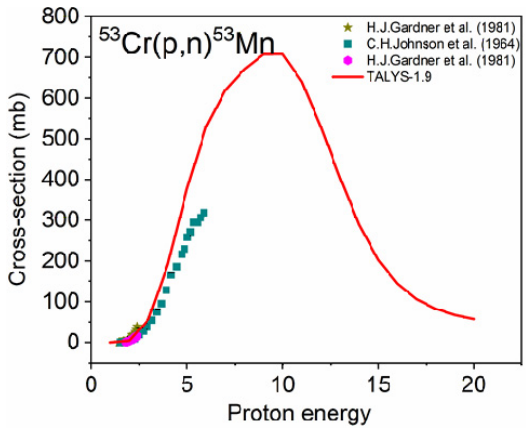

Figure 15. Calculated excitation function of $^{53}Cr(p,n)^{53}Mn$ along with experimental data.

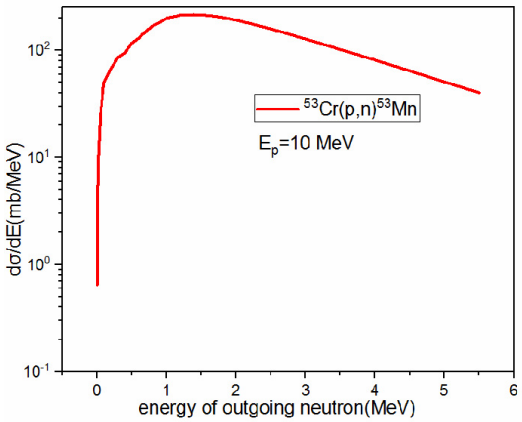

Figure 16. Calculated outgoing particle energy spectrum for $^{53}Cr(p,n)^{53}Mn$.

4. Summary and conclusions

The excitation functions ^{54}Fe(n,np)^{53}Mn, ^{54}Fe(n,2n)^{53}Fe(β^+)^{53}Mn, ^{54}Fe(n,d)^{53}Mn, ^{54}Mn(n,2n)^{53}Mn, ^{55}Fe(n,t)^{53}Mn and ^{57}Co(n,nα)^{53}Mn, ^{50}V(α,n)^{53}Mn, ^{53}Cr(p,n)^{53}Mn, ^{52}Cr(d,n)^{53}Mn for the production of ^{53}Mn have been calculated from threshold to 20 MeV using the TALYS-1.9 nuclear reaction modular models, with the following salient points:

- All the major pathways for the production of ^{53}Mn inside the fusion reactor have been studied;
- The contribution of sequential charged-particle reactions is quite high for the production of ^{53}Mn;
- Generally, charged-particle reactions are not taken into account during activation analysis for the production of long-lived radionuclides. The charged particle-induced inventory is therefore required as an addition to the presently available activation code, because any reaction channel implicating either neutron-induced or charged particle-induced (p,α,d) reactions can breed radionuclides during reactor operation. Inclusion of the charged particle inventory in the activation code would enable the real activation scenario to be completed;
- The present study highlights the need for the production cross-section of ^{53}Mn by charge particle-induced reactions experimentally as well as theoretically;
- There is a need to study the production cross-section of ^{53}Mn via neutron-induced reaction on unstable targets; i.e., ^{54}Mn(n,2n)^{53}Mn via an indirect (surrogate) method.

Acknowledgment

We thank the Board of Research in Nuclear Science for providing financial support under project no 39/14/09/2016-BRNS.

References

1. Fetter, S., Cheng, E.T. & Mann, F.M. Long-term radioactivity in fusion reactors. *Fusion Engng Design* **6** (1988) 123–130.
2. Pandey, B., Prajapati, P. M., Jakhar, S., Rao, C. V. S. & Basu T. K. Estimate of (n,p) cross-section for radionuclide ^{55}Fe Using EMPIRE and TALYS. *Nucl. Sci. Engng* **179** (2015) 313–320.
3. Pandey, J., Pandey, B., Agrawal, H.M., Subhash, P.V., Vala, S., Aiyyala, A.S., Makwana, R. & Suryanarayana, S.V. Estimation of (n, p) and (n,α) cross-section of radionuclide ^{60}Co for fusion technology applications. *Fusion Sci. Technol*. **73** (2018) 545–551.
4. Ojovan, M.I. & Lee, W.E. *An Introduction to Nuclear Waste Immobilisation* (2nd edn). Elsevier (2014).
5. Gilbert, M.R., Sublet, J.-C. & Forrest, R.A. *Handbook of activation, transmutation, and radiation damage properties of the elements simulated using FISPACT-II & TENDL-2014; Magnetic Fusion Plants (CCFE-R(15)26)*. Culham: Science Centre (2015).
6. Wallner, A., Buczak, K., Lederer, C., Vonach, H., Faestermann, T., Korschinek, G., Poutivtsev, M., Rugel, G., Klix, A., Seidel, K. & Plompen, A. Production of long-lived radionuclides ^{10}Be, ^{14}C, ^{53}Mn, ^{55}Fe, ^{59}Ni and ^{202g}Pb in a fusion environment. *J. Korean Phys. Soc.* **59** (2011) 1378–1381.
7. Forrest, R.A. Data requirements for neutron activation: Part I: Cross-sections. *Fusion Engng Design* **81** (2006) 2143–2156.
8. Cierjacks, S. & Hino, Y. The importance of sequential (x, n) reactions on element activation of fusion reactor materials. *J. Nucl. Mater.* **170** (1990) 134–139.

9. Hori, J.I., Ochiai, K., Sato, S., Yamauchi, M. & Nishitani, T. Sequential charged particle reaction, pp.27–30. (No. JAERI-REVIEW—2004-017) .
10. Koning, A.J., Hilaire, S. & Goriely, S. *TALYS-1.9: A Nuclear Reaction Program (User Manual)*. Petten, The Netherlands: NRG (2015).
11. Hauser, W. & Feshbach, H. The inelastic scattering of neutrons. *Phys. Rev*. **87** (1952) 366–373.
12. Capote, R., Herman, M., Obložinský, P., Young, P.G., Goriely, S., Belgya, T., Ignatyuk, A.V., Koning, A.J., Hilaire, S., Plujko, V.A. & Avrigeanu, M. RIPL—reference input parameter library for calculation of nuclear reactions and nuclear data evaluations. *Nucl. Data Sheets* **110** (2009) 3107–3214.